HHS Public Access

Author manuscript

ACS Biomater Sci Eng. Author manuscript; available in PMC 2023 March 31.

Published in final edited form as:

ACS Biomater Sci Eng. 2023 February 13; 9(2): 877–888. doi:10.1021/acsbiomaterials.2c01148.

Fibrin-Enriched Cardiac Extracellular Matrix Hydrogel Promotes *In Vitro* Angiogenesis

Rubia Shaik[‖],
Department of Biomedical Engineering, The University of Akron, Akron, Ohio 44325, United States

Jiazhu Xu[‖],
Department of Bioengineering, University of Texas at Arlington, Arlington, Texas 76019, United States

Yong Wang,
Department of Biomedical Engineering, Pennsylvania State University, University Park, Pennsylvania 16801, United States

Yi Hong,
Department of Bioengineering, University of Texas at Arlington, Arlington, Texas 76019, United States

Ge Zhang
Department of Biomedical Engineering, The University of Akron, Akron, Ohio 44325, United States

Abstract

Angiogenesis is essential for cardiac repair after myocardial infarction. Promoting angiogenesis has been demonstrated as an effective approach for myocardial infarction treatment. Several different strategies for inducing myocardial angiogenesis have been explored, including exogenous delivery of angiogenic genes, proteins, microRNAs, cells, and extracellular vesicles. Various types of injectable hydrogels have been investigated for cardiac tissue repair. One of the most promising injectable hydrogels in cardiac regeneration is a cardiac extracellular matrix hydrogel that is derived from decellularized porcine myocardium. It can be delivered minimally invasively *via* transendocardial delivery. The safety and efficacy of cardiac extracellular matrix hydrogels have been shown in small and large animal myocardial infarction models as well as clinical trials. The main mechanisms underlying the therapeutic benefits of cardiac extracellular matrix hydrogels have been elucidated and involved in the modulation of the immune response, downregulation

Corresponding Authors Yi Hong – Department of Bioengineering, University of Texas at Arlington, Arlington, Texas 76019, United States; Phone: 01-817-272-0562; yihong@uta.edu; **Ge Zhang** – Department of Biomedical Engineering, The University of Akron, Akron, Ohio 44325, United States; Phone: 01-330-972-5237; ge10@uakron.edu.

[‖]Author Contributions

R.S. and J.X. contributed equally to this work.

Supporting Information

The Supporting Information is available free of charge at https://pubs.acs.org/doi/10.1021/acsbiomaterials.2c01148.

Morphology and gelation kinetics of Fn hydrogels (Figure S1); comparison of network formation in Fn *vs* Fn-cECM hydrogels (Figure S2); the qualitative assessment of injectability of the hydrogels (Figure S3). (PDF)

The authors declare no competing financial interest.

of pathways related to heart failure progression and fibrosis, upregulation of genes important for cardiac muscle contraction, and enhancing cardiomyocyte differentiation and maturation from stem cells. However, no potent capillary network formation induced by cardiac extracellular matrix hydrogels has been reported. In this study, we tested the feasibility of incorporating a fibrin matrix into cardiac extracellular matrix hydrogels to improve the angiogenic properties of the hydrogel. Our *in vitro* results demonstrate that fibrin-enriched cardiac extracellular matrix hydrogels can induce robust endothelial cell tube formation from human umbilical vein endothelial cells and promote the sprouting of human mesenchymal stem cell spheroids. The obtained information from this study is very critical toward the future *in vivo* evaluation of fibrin-enriched cardiac extracellular matrix hydrogels in promoting myocardial angiogenesis.

Graphical Abstract

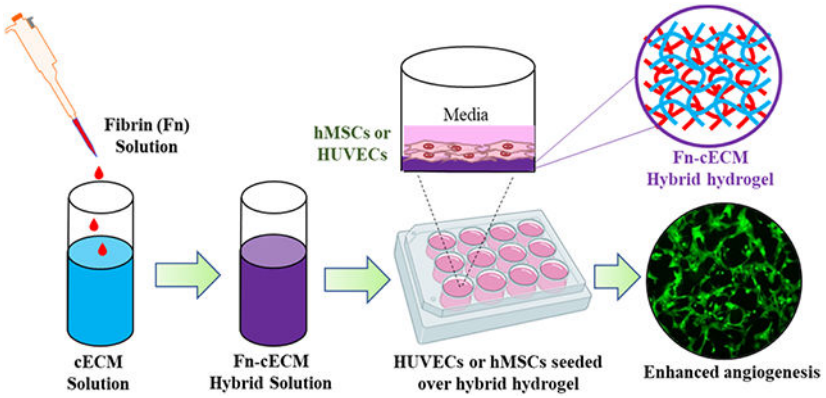

Keywords

cardiac extracellular matrix; fibrin; injectable hydrogel; angiogenesis assay; human umbilical vein endothelial cells; mesenchymal stem cells

1. INTRODUCTION

Promoting angiogenesis is one of the most effective strategies for improving the recovery of ventricular function after myocardial infarction (MI).[1-3] The root cause of MI is the reduced blood flow to the infarcted region, which restricts oxygen supply to the cardiomyocytes and ultimately leads to myocardial necrosis. Angiogenesis can improve revascularization, rescue dying cardiomyocytes, and reduce scarring and adverse left ventricular remodeling.[4-11] Furthermore, locally enhanced angiogenesis is a vital requirement for the long-term survival of therapeutic cells transplanted to an ischemic heart.[4,12,13] Several different strategies for inducing myocardial angiogenesis have been explored, including exogenous delivery of angiogenic genes, proteins, microRNAs, cells, and extracellular vesicles.[14-19] Successful preclinical studies and promising results of early clinical trials have demonstrated the great potential of myocardial angiogenesis for MI treatment.[20-23]

Injectable hydrogels have become a powerful tool to be exploited in minimally invasive, catheter-based heart procedures. Various types of injectable hydrogels have

been investigated for cardiac tissue repair.[24-26] For example, methacrylic anhydride (MA)–hyaluronic acid (HA) hydrogel has been used to deliver exosomes derived from human mesenchymal stem cells (MSCs) to the post-MI porcine heart through intrapericardial injection using a catheter.[27] Algisyl-LVR, a commercially available acellular alginate hydrogel, has been tested clinically in patients with MI and showed preservation of cardiac function after injection.[28] One of the most promising injectable hydrogels in cardiac regeneration is a cardiac extracellular matrix (cECM) hydrogel that is derived from decellularized porcine myocardium.[24,29,30] It can be delivered minimally invasively *via* transendocardial delivery.[31] The safety and efficacy of cECM have been tested using small and large animal MI models.[32] The outcomes of the recent phase 1 clinical trial support the safety and feasibility of injecting cECM hydrogels into post-MI patients and suggest the potential efficacy in chronic MI patients.[33] The main mechanisms underlying the therapeutic benefits of cECM hydrogels have been elucidated and involved in the modulation of the immune response, downregulation of pathways related to heart failure progression and fibrosis, and upregulation of genes important for cardiac muscle contraction.[34] *In vitro* studies also show that cECM hydrogels could enhance the differentiation and maturation of cardiomyocytes derived from pluripotent stem cells.[35,36] However, to date, there is no research evidence to suggest that cECM has a potent capability to induce capillary network formation.

In the present study, we aim to develop a proangiogenic cECM hydrogel for myocardial angiogenesis applications. We hypothesized that the incorporation of a fibrin matrix into cECM hydrogels would improve the angiogenic properties of the hydrogel. The role the fibrin matrix plays in stimulating and regulating angiogenesis has been extensively studied.[37-39] A large range of *in vitro* angiogenesis models have utilized the fibrin matrix as a culture system. When cultured on top or within a fibrin matrix, endothelial cells would rapidly form interconnecting capillary networks.[40,41] Here, we fabricated a hybrid hydrogel (Fn-cECM) by blending cECM with the fibrin matrix (Fn). We characterized the material properties of Fn-cECM hydrogels and compared them with those of cECM hydrogels. Using human umbilical vein endothelial cells (HUVECs) and human mesenchymal stem cells (hMSCs), we tested whether Fn-cECM hydrogels could induce *in vitro* angiogenesis without the addition of soluble factors. The obtained results are very critical to further optimize Fn-cECM hydrogels and evaluate their efficacy in promoting angiogenesis in MI models.

2. MATERIALS AND METHODS

2.1. Materials.

Human mesenchymal stem cells, human umbilical vein endothelial cells, EGM-2 BulletKit, 0.25% trypsin for hMSCs, and dissociation reagents kit for HUVECs (HBS, 0.25% trypsin, and TNS) were purchased from Lonza (Walkersville, MD). DMEM high in glucose with L-glutamine, fetal bovine serum, and penicillin–streptomycin were acquired from Gibco (Carlsbad, CA). Sodium dodecyl sulfate (SDS) was obtained from Bio-Rad (Hercules, CA). Pepsin, collagenase type-I, fibrinogen, tris-buffer saline, sodium hydroxide, thrombin, and calcium chloride were purchased from Sigma-Aldrich (St. Louis, MO). Dulbecco's phosphate-buffered saline (DPBS) was obtained from Corning Incorporated (Bedford, MA).

AggreWell400 24-well plates, antiadherence rinsing solution, and reversible cell strainer (37 μm) were obtained from StemCell Technologies (Vancouver, Canada). ELISA quantification kit and VEGF-A were purchased from R&D Systems (Minneapolis, MN). Paraformaldehyde (4%), Triton X-100, and goat serum were purchased from Thermo Fisher Scientific (Florence, KY). Anti-CD31, anti-vWF, and Alexa Fluor 488 and 647 were obtained from Abcam (Cambridge, MA). Calcein AM, Hoechst, and DAPI were acquired from Invitrogen (Waltham, MA).

2.2. Fabrication of Cardiac Extracellular Matrix Hydrogels.

Cardiac extracellular matrix (cECM) hydrogels were produced following a previously established protocol.[30,42] Briefly, fresh adult porcine hearts were obtained from a local USDA-approved butcher (Fischer's Meat Market and Grocery, Muenster, TX). The myocardium was isolated from the fresh whole heart after removing excessive vessels, fat, and connective tissues. The tissues were then sliced into 1 mm thick pieces and rinsed thoroughly with deionized (DI) water to remove blood, followed by decellularization with 1% SDS for 4 days with solution replaced with a fresh one every day.

The decellularized myocardial tissue was washed with excessive DI water overnight to completely remove SDS residue and then lyophilized. The lyophilized tissue was milled into a fine powder under liquid nitrogen and then enzymatically digested in 0.01 M hydrogen chloride (HCl) containing 1 mg/mL pepsin at room temperature for 24 h under constant stirring. After the powder was completely solubilized, 0.1 M sodium hydroxide (NaOH) and 10× PBS were added to adjust the pH to 7.4. The neutralized solution was diluted to desired concentration using 1× PBS and incubated at 37 °C to form cECM hydrogels.

2.3. Fabrication of Fibrin–Cardiac Extracellular Matrix Hybrid Hydrogels.

Fibrin–cardiac extracellular matrix hybrid (Fn-cECM) hydrogels were fabricated by blending the fibrin matrix (Fn) into cECM during hydrogel formation. Specifically, fibrinogen solution (100 mg/mL in tris-buffer saline) and thrombin (4 U/mL in 40 mM calcium chloride solution) were added to cECM pregel solution. The mixture was incubated at 37 °C to form Fn-cECM hydrogels. The final concentrations of fibrin (Fn) and cECM in the Fn-cECM hydrogel were 25 and 6.25 mg/mL, respectively.

2.4. Hydrogel Morphology.

The cardiac extracellular matrix (cECM), fibrin (Fn), and fibrin–cardiac extracellular matrix hybrid (Fn-cECM) were fractured after being frozen in liquid nitrogen and then lyophilized. The cross sections were sputter-coated with gold/platinum (Au/Pt) and then imaged with a scanning electron microscope (SEM, Hitachi, S-4800, Japan).

2.5. Turbidimetric Gelation Kinetics.

The gelation kinetics of cECM, Fn, and Fn-cECM hydrogels was studied turbidimetrically[43] using a Synergy H1 Hybrid microplate reader (BioTek) preheated to 37 °C. For each hydrogel, 100 μL was added in a 96-well plate in triplicate, and the absorbance was recorded at 405 nm every 2 mins over 60 mins. Normalized absorbance (NA) was calculated using the

equation NA = $(A - A_0)/(A_{max} - A_0)$, where A is the absorbance at a given time, A_0 is the initial absorbance, and A_{max} is the maximum absorbance.

2.6. Swelling Ratio and *In Vitro* Degradation.

The swelling ratio was evaluated following a previously published protocol.[44] Briefly, cECM (12.5 mg/mL) and Fn-cECM hydrogels were formed in 1 cm diameter steel rings and treated with 1× DPBS for 24 h at 37 °C. The swollen weight (W_s) was obtained, and then the hydrogels were air-dried at 40 °C for 24 h to determine the dry weight (W_d). The percentage swelling was calculated using the equation $(W_s - W_d)/W_d \times 100$. For studying enzymatic degradation, sample hydrogels were treated with collagenase type-I (250 U/mL) dissolved in 1× DPBS containing 0.9 mM $CaCl_2$ as previously described,[45-47] whereas control hydrogels were treated with 1× DPBS alone. Wet hydrogel weights of the sample (W_s) and control (W_c) were measured after 5 and 24 h of incubation at 37 °C. The percentage of remaining weight was calculated using the equation $(W_s/W_c) \times 100\%$. $n = 3$ for the two types of hydrogels at each time point.

2.7. Rheometric Analysis.

The mechanical properties of both cECM and Fn-cECM hydrogels were determined using a parallel plate rheometer (ARES RFS III). The pregel solutions were added into 1 cm diameter steel rings and incubated overnight at 37 °C. The following day, the hydrogels were subjected to mechanical testing, and the gap distance between the two parallel plates was maintained at 0.8 mm for all of the hydrogels. Dynamic frequency sweep tests were performed over a frequency range of 0.1 to 100 rad/s within the linear viscoelastic strain region of 1.5%, which was determined experimentally with a dynamic strain sweep test at a constant frequency of 0.5 rad/s. The storage modulus (G') determined from the dynamic frequency tests was reported over the range of 0.1–5 rad/s frequency. $n = 5$ for each type of hydrogel.

2.8. Culture of HUVECs and hMSCs.

Human umbilical vein endothelial cells (HUVECs) were cultured using an EGM-2 BulletKit supplemented with 1% penicillin–streptomycin (P/S) following the protocol provided by the manufacturer. Human mesenchymal stem cells (hMSCs) were cultured in DMEM supplemented with 10% fetal bovine serum (FBS) and 1% P/S at a seeding density of ~3,000 cells/cm^2. The cells were maintained in a humidified cell culture incubator at 37 °C and 5% CO_2, and the medium was replaced with a fresh one every other day for HUVECs and every 3 days for hMSCs. All experiments were performed using HUVECs at passages 2–4 and hMSCs at passage 5.

2.9. Cell Spheroid Formation.

hMSC spheroids were formed using AggreWell400 following the manufacturer's protocol. Briefly, each well of the AggreWell400 plate was rinsed with 500 μL of antiadherence rinsing solution at 1300 *g* for 5 min and then washed with 2 mL of warm DMEM basal medium. After prepping the plate, 0.6×10^6 cells/mL was added to each well (500 cells/microwell) with an additional 1 mL of medium, followed by centrifugation at 100 *g* for 3

min to evenly distribute the cells in all of the microwells. The cells were incubated at 37 °C for 5 days with 75% media changes performed every other day to form spheroids. After incubation, the spheroids were collected using a cell strainer.

2.10. *In Vitro* Angiogenesis Assay.

In vitro angiogenesis was performed using either cells or cell spheroids on two different substrates: cECM hydrogels and Fn-cECM hydrogels. First, a thin layer of either cECM or Fn-ECM hydrogels was formed inside of a 12-well plate by adding 19 μl (5 μL/cm^2) of pregel solution to each well that was evenly spread with the flat rubber end of the piston from a 1 mL BD syringe. Then, the cells or cell spheroids were seeded onto the thin layer of hydrogels at specific density (HUVECs: 1×10^5 cells/well; hMSCs: 3,000 cells/well; and hMSCs spheroids: 50 spheroids/well). After seeding, the cells and spheroids were cultured inside a cell culture incubator (Fisher Scientific Isotemp 3532 CO_2 Incubator) at 37 °C with 5% CO_2. Angiogenesis analysis was performed by staining the cells or cell spheroids using Calcein AM (2 μg/mL) and then analyzing the images by ImageJ software[48] with an angiogenesis analyzer plugin.[49]

2.11. Expression of Endothelial Cell Markers.

Immunofluorescence staining was used to confirm the expression of endothelial cell markers CD31, vWF, and VE-Cadherin. The cells or cell spheroids were fixed with 4% paraformaldehyde in 1× PBS solution at room temperature for 15 min, followed by permeabilization with 0.1% Triton X-100 in 1× DPBS for 15 min. They were then blocked with 10% goat serum for 1 h at room temperature. After the permeabilization and blocking steps, the cells or cell spheroids were incubated with primary antibodies CD31 (1:50), vWF (1:200), and VE-Cadherin (1:50) at 4 °C overnight. At the end of incubation, the samples were thoroughly washed with 1× DPBS and incubated with DAPI (12 μM/mL) and goat-derived secondary antibodies conjugated with Alexa Fluor 488 (1:500 for HUVECs and 1:100 for hMSCs spheroids), Alexa Fluor 647 (1:100 for HUVECs), and Alexa Fluor 594 (1:200 for hMSCs spheroids). HUVECs were treated with the secondary antibody for 2 h at room temperature, whereas hMSC spheroids were treated for 5 h. Next, the washing step was repeated, followed by fluorescence imaging with an inverted AxioVision A1 microscope (Carl Zeiss) for HUVECs and a Ti-E inverted microscope (Nikon A1 confocal) for imaging hMSC spheroids.

2.12. VEGF Secretion of hMSCs on Hydrogels.

The VEGF secreted by hMSCs seeded on the different types of hydrogels was quantified with an ELISA kit by following the manufacturer's protocol. For the quantification, about 150 μL of the hydrogel solutions was added into a 12-well plate and incubated at 37 °C overnight. The following day, 20,000 cells/mL was seeded in each well with an additional 1 mL medium and incubated at 37 °C. The medium was collected at the end of each time point, after which 2 mL of 250 U/mL collagenase type-1 was added to the wells and incubated at 37 °C for 24 h. The medium collected was centrifuged at 600 *g* for 5 min to discard any residual cells. The following day, the dissolved hydrogel solution was centrifuged and filtered with a 0.2 μm filter to remove debris. All of the samples ($n = 3$) collected over 21 days were tested for the amount of VEGF secreted using ELISA.

2.13. Statistical Analysis.

All of the data were reported as means ± SD with 3–10 independent samples. The statistical analysis was performed using GraphPad Prism 9. Comparison of two groups was performed with the unpaired, two-tailed Student's *t*-test, while for multiple groups, two-tailed two-way ANOVA was performed with Tukey's post hoc test. The data were considered statistically significant for a *p*-value less than 0.05.

3. RESULTS

3.1. Morphology and Gelation Time of Fn-cECM Hydrogels.

The Fn-cECM hydrogel fabrication process was determined by tuning the concentrations of fibrinogen, thrombin, and cECM solutions during the blending process. Various concentrations of fibrinogen (from 12.5 to 100 mg/mL), thrombin (1, 2, and 4 U/mL), and cECM solution (from 1 to 12.5 mg/mL) were tested, and the gelation times of the formed hydrogels were measured. For our chosen combination of solution concentrations, the gelation time was ~30 min, which is in the range of catheter-deliverable hydrogels.[50-52] Compared with the cECM hydrogel that looks slightly translucent at the same concentration, the Fn-cECM hydrogel looks opaque with well-rounded edges (Figure 1A). SEM images showed that cECM hydrogels have a nanofibrous network with some sheets and that fibrin hydrogels have a general fibrous structure (see the Supporting Information). The Fn-cECM hydrogel also has a combination of nanofibers and sheets that appear much similar to the cECM hydrogel (Figure 1A). The gelation kinetic data demonstrate that Fn-cECM solution starts transitioning into a gel state faster than cECM solution (Figure 1B). The cECM hydrogel gelation curve has a typical sigmoidal shape, and the gelation started after a lag phase (T_{lag} = 13.33 ± 1.15 min), whereas the gelation kinetic curve of Fn-cECM does not have any lag phase (T_{lag} = 0) (Figure 1C). The time to reach 50% gelation ($T_{1/2}$) for cECM hydrogels was 17.67 ± 1.15 min and 12.67 ± 0.58 min for Fn-cECM hydrogels.

3.2. Mechanical Properties, *In Vitro* Swelling, and Degradation of Fn-cECM Hydrogels.

The storage moduli (G') and complex moduli (G^*) of Fn-cECM hydrogels were measured and compared with cECM hydrogels. Both G' and G^* of Fn-cECM hydrogels were significantly higher than those of cECM hydrogels (897 ± 110 Pa *vs* 138 ± 27 Pa for G'; 915 ± 111 Pa *vs* 140 ± 27 Pa for G^*) (Figure 2A,B). The swelling behavior of the hydrogels was studied *in vitro*. Figure 2C shows that the swelling ratio of Fn-cECM (3545 ± 285%) was significantly lower than that of cECM (5152 ± 94%). The transition from the dry state into hydrogels increased the mass of Fn-cECM by over 35 times and that of cECM by over 50 times. The enzymatic degradation of Fn-cECM and cECM hydrogels was examined. As shown in Figure 2D, there was no significant difference between the percentage of weight remaining for cECM and Fn-cECM hydrogels after 5 h immersion in collagenase solution. However, after 24 h, only 28 ± 6.27% of Fn-cECM hydrogels remained, which is significantly less than that of cECM hydrogels.

3.3. Fn-cECM Hydrogel Induces Endothelial Cell Tube Formation.

To test the proangiogenic capacity of Fn-cECM, we performed a tube formation assay. After 16 h of seeding HUVECs onto Fn-cECM hydrogels, extensive tubelike structures formed and linked with each other to form networks (Figure 3A). Strong expression of endothelial cell markers CD31 and VWF are detected (Figure 3B,C). HUVECs also attached to cECM hydrogels and expressed endothelial cell markers after seeding, but only a small percentage of cells could form vascular networks (Figure 3D-F). Image analysis results confirm that Fn-cECM induces a higher level of endothelial cell tube formation evidenced by forming a higher number of nodes, tubes, total tube length, meshes, mean mesh size, and total mesh area when compared with cECM hydrogels (Figure 3G). Similarly, HUVECs also formed networks on fibrin (Fn) hydrogels; however, they were not as prominent as those on Fn-cECM hydrogels (see the Supporting Information).

3.4. Fn-cECM Hydrogel Interacts with hMSCs.

Similar to the effects on HUVECs, Fn-cECM hydrogels also induce more robust tube network formation of seeded hMSCs compared with cECM hydrogels (Figure 4A,B). The difference between the number of nodes, tubes, total tube length, meshes, and total mesh area derived from the networks formed on the two types of hydrogels is still significant (Figure 4C). However, less fold changes of these parameters are observed when compared with seeding with hMSCs instead of HUVECs on Fn-cECM and cECM hydrogels. For example, the average tube number of HUVECs increased 4-fold when cultured on Fn-cECM hydrogels other than cECM hydrogels, while it only increased 1.5-fold for hMSCs. There is no significant difference in the mean mesh size on the two types of hydrogels. In addition, no detectable expressions of CD31 and VWF were found on the cells forming networks on Fn-cECM hydrogels. We also measured VEGF secreted from the hMSCs seeded on the two types of hydrogels for up to 21 days (Figure 4D). It is noticeable that beginning from day 14, more VEGF was secreted by the hMSCs seeded on Fn-cECM hydrogel.

3.5. Fn-cECM Hydrogel Promotes Sprouting of hMSC Spheroids.

Since we did not detect the expressions of CD31 and vWF for hMSCs seeded on Fn-cECM, we examined whether a three-dimensional (3D) culture would affect the response of hMSCs to Fn-cECM hydrogels. We performed an *in vitro* spheroid sprouting assay to test the influence of Fn-cECM hydrogels on 3D-cultured hMSCs. After 24 h of seeding hMSC spheroids on either cECM or Fn-cECM hydrogels, we observed the formation of sprout structures on both hydrogel types with a distinct pattern (Figure 5A,B). The tip cells of spheroids on cECM hydrogels formed short sprouts with weak interactions, while on Fn-cECM hydrogels, the tip cells formed well-defined sprouts with long capillary-like structures. Further quantitative assessment confirmed that hMSC spheroids cultured on Fn-cECM hydrogels had more sprouts coming out of the spheroids (Figure 5C). The average and cumulative sprouting lengths of the sprouts grown on Fn-cECM hydrogels were also significantly longer (Figure 5D,E). The spheroid area, which is defined as the area covered by the core of the spheroid for both hydrogel types, did not show a statistically significant difference (Figure 5F). However, the spheroid sprouting area, which is the total area covered by sprouts only, was significantly higher for Fn-cECM hydrogels (Figure 5G).

3.6. Fn-cECM Hydrogel Enhances Endothelial Differentiation of hMSC Spheroids.

To verify whether the sprouting structures we observed from the *in vitro* spheroid sprouting assay are angiogenic sprouting, we stained the samples with endothelial cell markers CD31 and VE-Cadherin. As shown in Figure 6A,B, we detected $CD31^+$ and VE-$Cadherin^+$ endothelial cell populations in hMSC spheroids cultured in hMSC cell culture medium. Most of the VE-Cadherin-expressing cells were located near the edge of the spheroids. There are more cells expressing CD31 than VE-Cadherin within the spheroids when they are cultured in the medium. When cultured on cECM hydrogels and Fn-cECM hydrogels, more cells not only within spheroids but also in sprouting structures express CD31 (Figure 6C,E). The VE-$Cadherin^+$ endothelial cells dramatically increased in the center area of the spheroids when cultured on Fn-cECM hydrogels (Figure 6B,D,F).

4. DISCUSSION

The motivation of this study is to develop an injectable hydrogel for cardiac tissue repair by enhancing the benefits of hydrogels derived from decellularized cardiac ECM tissue with the angiogenic properties of fibrin. Both cECM and fibrin hydrogels are very promising biomaterials that provide numerous advantages in functioning as tissue engineering scaffolds and cell delivery platforms for treating injured myocardium.[53-56] Both are natural materials, fully degradable, and favor cell interactions.[57-59] In addition, each of them has unique features enabling their cardiac applications. The most appealing features of cECM hydrogels are as follows: (1) retaining cardiac tissue-specific ECM composition; (2) serving as a reservoir for anchored cytokines and growth factors; and (3) demonstrating safety in minimally invasive intramyocardial delivery through a catheter in a clinical setting.[60,61] Unlike the cECM hydrogel, which is an emerging biomaterial, fibrin is one of the classical and well-known biomaterials that has been widely used for many applications.[62-65] One well-proven benefit of fibrin hydrogels is that they can promote angiogenesis (see the Supporting Information Figure S2). It has been reported that fibrin hydrogels led to endothelial assembly into microvessels and angiogenic sprouting both *in vitro* and *in vivo*.[66,67] In this study, we demonstrate the feasibility of physically blending cECM and fibrin to form an injectable hydrogel with potential for cardiac applications. It needs to be noted that another research group also investigated developing a hybrid of cECM and fibrin, but the reported fabrication process requires additional crosslinkers, *e.g.,* transglutaminase (TG), to achieve the desired mechanical properties. Furthermore, the research focus is to investigate how stiffness and ECM composition of the cECM and fibrin hybrid affect cardiovascular differentiation of cardiac progenitor cells,[68] while ours aims to optimize hydrogel properties to promote angiogenesis.

Our obtained results suggest that the incorporation of a fibrin matrix into cECM hydrogels has multifaceted effects on hydrogel material properties. First, it enables the tuning of hydrogel gelation to be more favorable for our intended cardiac applications. cECM and Fn hydrogels have distinct gelation curves. The gelling behavior of Fn-cECM hydrogels follows the same pattern as Fn hydrogels (see the Supporting Information Figure S1) with accelerated gelation compared with cECM hydrogels. The Fn-cECM hydrogel we developed has the gelation kinetics that enables sufficient time to mix pregel solutions and pass the

solution mixture through a catheter and timely transition to gel after delivery. Second, the incorporation of a fibrin matrix into cECM hydrogels increases mechanical stiffness and reduces the swelling of the hydrogel, which are beneficial to provide mechanical support for damaged cardiac tissue and avoid heart wall disruption after hydrogel injection. Many studies have demonstrated that the mechanical properties of substrate would affect cell behaviors. For example, endothelial cell spreading and extension formation increase with matrix stiffness.[69] Our study also confirmed that Fn-cECM hydrogels induced higher levels of tube network formation due to their higher mechanical strength compared to cECM hydrogels.

Third, we noticed that Fn-cECM hydrogels degraded significantly faster than cECM hydrogels when treated with collagenase solution for 24 h. Although the reason that causes the rapid enzymatic degradation is unclear, it can be a potential drawback in using Fn-cECM hydrogels in cardiac treatment. We will examine the *in vivo* degradation rate of Fn-cECM hydrogels in our future animal studies and further modify it by adding MMP inhibitors such as doxycycline when necessary.[70] Last but most importantly, the incorporation of a fibrin matrix into cECM hydrogels enhanced the proangiogenic properties of the hydrogel. Our results demonstrate that Fn-cECM hydrogels promote rapid and robust vascular network formation of HUVECs, which have not been observed in cECM hydrogels *in vitro*.

Our results prove that blending Fn could be a simple and effective strategy to enhance the angiogenic properties of existing hydrogels. This strategy has been explored by several research groups with other types of hydrogels.[71-75] For example, a collagen/fibrin mixed construct containing HUVECs has been shown to induce lumen formation 7 days after being implanted subcutaneously in mice.[76] Blending fibrin in a composite hydrogel containing alginate and iron nanoparticles has been reported to enhance the attachment of endothelial cells and promote strong endothelization.[77] With the increasing interest in utilizing organ-specific ECM hydrogels for disease treatment and the critical role angiogenesis plays in tissue repair, we expect the approach in this study can be readily adopted by many researchers to benefit a broader scientific community.

We also evaluated the response of MSCs to Fn-cECM hydrogels to test whether the proangiogenic feature of our hydrogel could induce endothelial differentiation of MSCs. MSCs are one of the most popular cell types used in cardiac cell therapy.[78-80] Many completed and ongoing clinical trials have been conducted to investigate the efficacy of MSCs in MI treatment.[81-88] The therapeutic effects of MSCs include their ability to differentiate into cardiovascular cells, immunomodulatory properties, antifibrotic activity, and ability to undergo neovasculogenesis.[89-92] In this study, the distinct effects of Fn-cECM on MSCs and MSC spheroids are identified. Fn-cECM could cause morphological alteration of MSCs toward vascular tube formation and VEGF secretion but is insufficient in directing them to express endothelial cell-specific markers. However, when it acts on MSC spheroids, it could not only enhance angiogenic sprouting but also upregulate the expression of endothelial cell-specific markers of cells in MSC spheroids. We observe that culturing MSCs in 3D as spheroid triggers their differentiation toward endothelial cells. The synergy between 3D culture and Fn-cECM hydrogels facilitates the endothelial differentiation process and promotes sprouting angiogenesis. These findings suggest the potential use of Fn-cECM

hydrogels to deliver MSC spheroids to increase MSC functionalization for enhanced therapeutic applications.

Although the developed Fn-cECM hydrogel demonstrated enhanced material properties and improved angiogenic capacity, there are some issues that could potentially affect its successful application in myocardial infarction treatment. The Fn-cECM hydrogel is injectable (see the Supporting Information), but whether it is compatible with catheter delivery in a clinical setting is unknown. The Fn-cECM hydrogel is degradable. Its *in vivo* degradation rate would affect the therapeutic outcomes and should be carefully examined. In this study, we used a 2D angiogenesis assay by seeding the cells and cell spheroids on the hydrogels to test the angiogenic properties of Fn-cECM hydrogel. Although the 2D angiogenesis assay is widely used by biomaterials researchers and has many advantages, the cells seeded on the hydrogel and encapsulated inside the hydrogel may respond differently. In our future studies, we will perform a 3D angiogenesis assay to further investigate the effects of Fn-cECM hydrogel on encapsulated cells and conduct *in vivo* study to investigate the feasibility and efficacy of using the developed Fn-cECM hydrogel to promote myocardial angiogenesis.

5. CONCLUSIONS

In this study, we presented the development of a proangiogenic cECM hydrogel. We demonstrated the feasibility of incorporating a fibrin matrix into cECM hydrogels by blending. We have found that our developed Fn-cECM hydrogel has accelerated gelation and improved mechanical properties. We confirmed that Fn-cECM hydrogels promote *in vitro* angiogenesis through a vascular tube formation assay. Additionally, we found that Fn-cECM hydrogels increase the secretion of VEGF of MSCs and enhance the angiogenic sprouting of MSC spheroids. The approach we exploited in this study is a simple and effective strategy to enhance the angiogenic properties of existing hydrogels.

Supplementary Material

Refer to Web version on PubMed Central for supplementary material.

ACKNOWLEDGMENTS

This work was partially supported by the National Institutes of Health (R15HL140503 and R01HL 122311).

REFERENCES

(1). Cochain C; Channon KM; Silvestre JS Angiogenesis in the Infarcted Myocardium. Antioxid. Redox Signaling 2013, 18, 1100–1113.

(2). Liao YY; Chen ZY; Wang YX; Lin Y; Yang F; Zhou QL New Progress in Angiogenesis Therapy of Cardiovascular Disease by Ultrasound Targeted Microbubble Destruction. BioMed Res. Int 2014, 2014, No. 872984. [PubMed: 24900995]

(3). Shi W; Xin Q; Yuan R; Yuan Y; Cong W; Chen K Neovascularization: The Main Mechanism of MSCs in Ischemic Heart Disease Therapy. Front. Cardiovasc. Med 2021, 8, No. 633300. [PubMed: 33575274]

(4). Johnson T; Zhao L; Manuel G; Taylor H; Liu D Approaches to Therapeutic Angiogenesis for Ischemic Heart Disease. J. Mol. Med 2019, 97, 141–151. [PubMed: 30554258]

(5). Li J; Zhao Y; Zhu W Targeting Angiogenesis in Myocardial Infarction: Novel Therapeutics (Review). Exp. Ther. Med 2021, 23, No. 64. [PubMed: 34934435]

(6). Zhang Q; Wang L; Wang S; Cheng H; Xu L; Pei G; Wang Y; Fu C; Jiang Y; He C; Wei Q Signaling Pathways and Targeted Therapy for Myocardial Infarction. Signal Transduction Targeted Ther. 2022, 7, No. 78.

(7). Marín-Juez R; Marass M; Gauvrit S; Rossi A; Lai SL; Materna SC; Black BL; Stainier DYR Fast Revascularization of the Injured Area is Essential to Support Zebrafish Heart Regeneration. Proc. Natl. Acad. Sci. U.S.A 2016, 113, 11237–11242. [PubMed: 27647901]

(8). Gordon O; Gilon D; He Z; May D; Lazarus A; Oppenheim A; Keshet E Vascular Endothelial Growth Factor-induced Neovascularization Rescues Cardiac Function but not Adverse Remodeling at Advanced Ischemic Heart Disease. Arterioscler., Thromb., Vasc. Biol 2012, 32, 1642–1651. [PubMed: 22539593]

(9). Awada HK; Hwang MP; Wang Y Towards Comprehensive Cardiac Repair and Regeneration after Myocardial Infarction: Aspects to Consider and Proteins to Deliver. Biomaterials 2016, 82, 94–112. [PubMed: 26757257]

(10). Cahill TJ; Choudhury RP; Riley PR Heart Regeneration and Repair after Myocardial Infarction: Translational Opportunities for Novel Therapeutics. Nat. Rev. Drug Discovery 2017, 16, 699–717. [PubMed: 28729726]

(11). Nakamura Y; Asakura Y; Piras BA; Hirai H; Tastad CT; Verma M; Christ AJ; Zhang J; Yamazaki T; Yoshiyama M; Asakura A Increased Angiogenesis and Improved Left Ventricular Function after Transplantation of Myoblasts Lacking the MyoD Gene into Infarcted Myocardium. PLoS One 2012, 7, No. e41736. [PubMed: 22848585]

(12). Bhang SH; Cho SW; Lim JM; Kang JM; Lee TJ; Yang HS; Song YS; Park MH; Kim HS; Yoo KJ; Jang Y; Langer R; Anderson DG; Kim BS Locally Delivered Growth Factor Enhances the Angiogenic Efficacy of Adipose-derived Stromal Cells Transplanted to Ischemic Limbs. Stem Cells 2009, 27, 1976–1986. [PubMed: 19544425]

(13). Ruan L; Wang B; ZhuGe Q; Jin K Coupling of Neurogenesis and Angiogenesis after Ischemic Stroke. Brain Res. 2015, 1623, 166–173. [PubMed: 25736182]

(14). Zhang J; Ding L; Zhao Y; Sun W; Chen B; Lin H; Wang X; Zhang L; Xu B; Dai J Collagen-targeting Vascular Endothelial Growth Factor Improves Cardiac Performance after Myocardial Infarction. Circulation 2009, 119, 1776–1784. [PubMed: 19307480]

(15). Lähteenvuo JE; Lähteenvuo MT; Kivelä A; Rosenlew C; Falkevall A; Klar J; Heikura T; Rissanen TT; Vähäkangas E; Korpisalo P; Enholm B; Carmeliet P; Alitalo K; Eriksson U; Ylä-Herttuala S Vascular Endothelial Growth Factor-B Induces Myocardium-specific Angiogenesis and Arteriogenesis Via Vascular Endothelial Growth Factor Receptor-1- and Neuropilin Receptor-1-Dependent Mechanisms. Circulation 2009, 119, 845–856. [PubMed: 19188502]

(16). Orlic D; Kajstura J; Chimenti S; Jakoniuk I; Anderson SM; Li B; Pickel J; McKay R; Nadal-Ginard B; Bodine DM; Leri A; Anversa P Bone Marrow Cells Regenerate Infarcted Myocardium. Nature 2001, 410, 701–705. [PubMed: 11287958]

(17). KC P; Shah M; Shaik R; Hong Y; Zhang G Preseeding of Mesenchymal Stem Cells Increases Integration of an iPSC-Derived CM Sheet into a Cardiac Matrix. ACS Biomater. Sci. Eng 2020, 6, 6808–6818. [PubMed: 33320624]

(18). Ma T; Chen Y; Chen Y; Meng Q; Sun J; Shao L; Yu Y; Huang H; Hu Y; Yang Z; Yang J; Shen Z MicroRNA-132, Delivered by Mesenchymal Stem Cell-Derived Exosomes, Promote Angiogenesis in Myocardial Infarction. Stem Cells Int. 2018, 2018, No. 3290372. [PubMed: 30271437]

(19). Gallet R; Dawkins J; Valle J; Simsolo E; de Couto G; Middleton R; Tseliou E; Luthringer D; Kreke M; Smith RR; Marbán L; Ghaleh B; Marbán E Exosomes Secreted by Cardiosphere-derived Cells Reduce Scarring, Attenuate Adverse Remodelling, and Improve Function in Acute and Chronic Porcine Myocardial Infarction. Eur. Heart J 2017, 38, 201–211. [PubMed: 28158410]

(20). Kobayashi K; Maeda K; Takefuji M; Kikuchi R; Morishita Y; Hirashima M; Murohara T Dynamics of Angiogenesis in Ischemic Areas of the Infarcted Heart. Sci. Rep 2017, 7, No. 7156. [PubMed: 28769049]

(21). Ferraro B; Leoni G; Hinkel R; Ormanns S; Paulin N; Ortega-Gomez A; Viola JR; de Jong R; Bongiovanni D; Bozoglu T; Maas SL; D'Amico M; Kessler T; Zeller T; Hristov M; Reutelingsperger C; Sager HB; Döring Y; Nahrendorf M; Kupatt C; Soehnlein O Pro-Angiogenic Macrophage Phenotype to Promote Myocardial Repair. J. Am. Coll. Cardiol 2019, 73, 2990–3002. [PubMed: 31196457]

(22). Laham RJ; Sellke FW; Edelman ER; Pearlman JD; Ware JA; Brown DL; Gold JP; Simons M Local Perivascular Delivery of Basic Fibroblast Growth Factor in Patients Undergoing Coronary Bypass Surgery: Results of a Phase I Randomized, Double-blind, Placebo-controlled Trial. Circulation 1999, 100, 1865–1871. [PubMed: 10545430]

(23). Rosengart TK; Bishawi MM; Halbreiner MS; Fakhoury M; Finnin E; Hollmann C; Shroyer AL; Crystal RG Long-term Follow-up Assessment of a Phase 1 Trial of Angiogenic Gene Therapy using Direct Intramyocardial Administration of an Adenoviral Vector Expressing the VEGF121 cDNA for the Treatment of Diffuse Coronary Artery Disease. Hum. Gene Ther 2013, 24, 203–208. [PubMed: 23137122]

(24). Hasan A; Khattab A; Islam MA; Hweij KA; Zeitouny J; Waters R; Sayegh M; Hossain MM; Paul A Injectable Hydrogels for Cardiac Tissue Repair after Myocardial Infarction. Adv. Sci 2015, 2, No. 1500122.

(25). Tan H; Marra KG Injectable, Biodegradable Hydrogels for Tissue Engineering Applications. Materials 2010, 3, 1746–1767.

(26). Peña B; Laughter M; Jett S; Rowland TJ; Taylor MRG; Mestroni L; Park D Injectable Hydrogels for Cardiac Tissue Engineering. Macromol. Biosci 2018, 18, No. 1800079.

(27). Zhu D; Li Z; Huang K; Caranasos TG; Rossi JS; Cheng K Minimally Invasive Delivery of Therapeutic Agents by Hydrogel Injection into the Pericardial Cavity for Cardiac Repair. Nat. Commun 2021, 12, No. 1412. [PubMed: 33658506]

(28). Cattelan G; Gerbolés AG; Foresti R; Pramstaller PP; Rossini A; Miragoli M; Malvezzi CC Alginate Formulations: Current Developments in the Race for Hydrogel-Based Cardiac Regeneration. Front. Bioeng. Biotechnol 2020, 8, No. 414. [PubMed: 32457887]

(29). KC P; Hong Y; Zhang G Cardiac Tissue-derived Extracellular Matrix Scaffolds for Myocardial Repair: Advantages and Challenges. Regener. Biomater 2019, 6, 185–199.

(30). Mulvany E; McMahan S; Xu J; Yazdani N; Willits R; Liao J; Zhang G; Hong Y In Vitro Comparison of Harvesting Site Effects on Cardiac Extracellular Matrix Hydrogels. J. Biomed. Mater. Res., Part A 2021, 109, 1922–1930.

(31). Seif-Naraghi SB; Singelyn JM; Salvatore MA; Osborn KG; Wang JJ; Sampat U; Kwan OL; Strachan GM; Wong J; Schup-Magoffin PJ; Braden RL; Bartels K; DeQuach JA; Preul M; Kinsey AM; DeMaria AN; Dib N; Christman KL Safety and Efficacy of an Injectable Extracellular Matrix Hydrogel for Treating Myocardial Infarction. Sci. Transl. Med 2013, 5, No. 173ra25.

(32). Wassenaar JW; Gaetani R; Garcia JJ; Braden RL; Luo CG; Huang D; DeMaria AN; Omens JH; Christman KL Evidence for Mechanisms Underlying the Functional Benefits of a Myocardial Matrix Hydrogel for Post-MI Treatment. J. Am. Coll. Cardiol 2016, 67, 1074–1086. [PubMed: 26940929]

(33). Traverse JH; Henry TD; Dib N; Patel AN; Pepine C; Schaer GL; DeQuach JA; Kinsey AM; Chamberlin P; Christman KL First-in-Man Study of a Cardiac Extracellular Matrix Hydrogel in Early and Late Myocardial Infarction Patients. JACC: Basic Transl. Sci 2019, 4, 659–669. [PubMed: 31709316]

(34). Diaz MD; Tran E; Spang M; Wang R; Gaetani R; Luo CG; Braden R; Hill RC; Hansen KC; DeMaria AN; Christman KL Injectable Myocardial Matrix Hydrogel Mitigates Negative Left Ventricular Remodeling in a Chronic Myocardial Infarction Model. JACC: Basic Transl. Sci 2021, 6, 350–361. [PubMed: 33997521]

(35). Fong AH; Romero-López M; Heylman CM; Keating M; Tran D; Sobrino A; Tran AQ; Pham HH; Fimbres C; Gershon PD; Botvinick EL; George SC; Hughes CCW Three-Dimensional Adult Cardiac Extracellular Matrix Promotes Maturation of Human Induced Pluripotent Stem Cell-Derived Cardiomyocytes. Tissue Eng., Part A 2016, 22, 1016–1025. [PubMed: 27392582]

(36). Xiao X; Wang M; Qiu X; Ling W; Chu X; Huang Y; Li T Construction of Extracellular Matrix-based 3D Hydrogel and its Effects on Cardiomyocytes. Exp. Cell Res 2021, 408, No. 112843. [PubMed: 34563515]

(37). Ahmed TA; Dare EV; Hincke M Fibrin: A Versatile Scaffold for Tissue Engineering Applications. Tissue Eng., Part B 2008, 14, 199–215.

(38). Tonnesen MG; Feng X; Clark RAF Angiogenesis in Wound Healing. J. Invest. Dermatol. Symp. Proc 2000, 5, 40–46.

(39). Barsotti MC; Felice F; Balbarini A; Di Stefano R Fibrin as a Scaffold for Cardiac Tissue Engineering. Biotechnol. Appl. Biochem 2011, 58, 301–310. [PubMed: 21995533]

(40). Annamalai RT; Rioja AY; Putnam AJ; Stegemann JP Vascular Network Formation by Human Microvascular Endothelial Cells in Modular Fibrin Microtissues. ACS Biomater. Sci. Eng 2016, 2, 1914–1925. [PubMed: 29503863]

(41). Rioja AY; Annamalai RT; Paris S; Putnam AJ; Stegemann JP Endothelial Sprouting and Network Formation in Collagen- and Fibrin-based Modular Microbeads. Acta Biomater. 2016, 29, 33–41. [PubMed: 26481042]

(42). Singelyn JM; DeQuach JA; Seif-Naraghi SB; Littlefield RB; Schup-Magoffin PJ; Christman KL Naturally Derived Myocardial Matrix as an Injectable Scaffold for Cardiac Tissue Engineering. Biomaterials 2009, 30, 5409–5416. [PubMed: 19608268]

(43). Wolf MT; Daly KA; Brennan-Pierce EP; Johnson SA; Carruthers CA; D'Amore A; Nagarkar SP; Velankar SS; Badylak SF A Hydrogel Derived from Decellularized Dermal Extracellular Matrix. Biomaterials 2012, 33, 7028–7038. [PubMed: 22789723]

(44). Jeffords ME; Wu J; Shah M; Hong Y; Zhang G Tailoring Material Properties of Cardiac Matrix Hydrogels to Induce Endothelial Differentiation of Human Mesenchymal Stem Cells. ACS Appl. Mater. Interfaces 2015, 7, 11053–11061. [PubMed: 25946697]

(45). Lee SH; Moon JJ; Miller JS; West JL Poly(ethylene glycol) Hydrogels Conjugated with a Collagenase-sensitive Fluorogenic Substrate to Visualize Collagenase Activity during Three-dimensional Cell Migration. Biomaterials 2007, 28, 3163–3170. [PubMed: 17395258]

(46). Macaya D; Ng KK; Spector M Injectable Collagen-Genipin Gel for the Treatment of Spinal Cord Injury: In Vitro Studies. Adv. Funct. Mater 2011, 21, 4788–4797.

(47). Ong SR; Trabbic-Carlson KA; Nettles DL; Lim DW; Chilkoti A; Setton LA Epitope Tagging for Tracking Elastin-like Polypeptides. Biomaterials 2006, 27, 1930–1935. [PubMed: 16278015]

(48). Rasband WS Image J; U. S. National Institutes of Health: Bethesda, Maryland, USA, 2020.

(49). Carpentier G Angiogenesis Analyzer for ImageJ; ImageJ News, 2012, November 9, 2012.

(50). Singelyn JM; Sundaramurthy P; Johnson TD; Schup-Magoffin PJ; Hu DP; Faulk DM; Wang J; Mayle KM; Bartels K; Salvatore M; Kinsey AM; Demaria AN; Dib N; Christman KL Catheter-deliverable Hydrogel Derived from Decellularized Ventricular Extracellular Matrix Increases Endogenous Cardiomyocytes and Preserves Cardiac Function Post-Myocardial Infarction. J. Am. Coll. Cardiol 2012, 59, 751–763. [PubMed: 22340268]

(51). Pape ACH; Bakker MH; Tseng CCS; Bastings MMC; Koudstaal S; Agostoni P; Chamuleau SAJ; Dankers PYW An Injectable and Drug-loaded Supramolecular Hydrogel for Local Catheter Injection into the Pig Heart. J. Visualized Exp 2015, 100, No. e52450.

(52). Mathieu E; Lamirault G; Toquet C; Lhommet P; Rederstorff E; Sourice S; Biteau K; Hulin P; Forest V; Weiss P; Guicheux J; Lemarchand P Intramyocardial Delivery of Mesenchymal Stem Cell-seeded Hydrogel Preserves Cardiac Function and Attenuates Ventricular Remodeling after Myocardial Infarction. PLoS One 2012, 7, No. e51991. [PubMed: 23284842]

(53). Wang RM; Christman KL Decellularized Myocardial Matrix Hydrogels: In Basic Research and Preclinical Studies. Adv. Drug Delivery Rev 2016, 96, 77–82.

(54). Yang X; Chen S; Chen J; Liu Y; Bai Y; Yin S; Quan D The Different Effect of Decellularized Myocardial Matrix Hydrogel and Decellularized Small Intestinal Submucosa Matrix Hydrogel on Cardiomyocytes and Ischemic Heart. Appl. Sci 2021, 11, No. 7768.

(55). Ryu JH; Kim I-K; Cho S-W; Cho M-C; Hwang K-K; Piao H; Piao S; Lim SH; Hong YS; Choi CY; Yoo KJ; Kim BS Implantation of Bone Marrow Mononuclear Cells using Injectable Fibrin Matrix Enhances Neovascularization in Infarcted Myocardium. Biomaterials 2005, 26, 319–326. [PubMed: 15262474]

(56). Christman KL; Vardanian AJ; Fang Q; Sievers RE; Fok HH; Lee RJ Injectable Fibrin Scaffold Improves Cell Transplant Survival, Reduces Infarct Expansion, and Induces Neovasculature Formation in Ischemic Myocardium. J. Am. Coll. Cardiol 2004, 44, 654–660. [PubMed: 15358036]

(57). Li Y; Meng H; Liu Y; Lee BP Fibrin Gel as an Injectable Biodegradable Scaffold and Cell Carrier for Tissue Engineering. Sci. World J 2015, 2015, No. 685690.

(58). Thomson KS; Korte FS; Giachelli CM; Ratner BD; Regnier M; Scatena M Prevascularized Microtemplated Fibrin Scaffolds for Cardiac Tissue Engineering Applications. Tissue Eng., Part A 2013, 19, 967–977. [PubMed: 23317311]

(59). Pok S; Benavides OM; Hallal P; Jacot JG Use of Myocardial Matrix in a Chitosan-based Full-thickness Heart Patch. Tissue Eng., Part A 2014, 20, 1877–1887. [PubMed: 24433519]

(60). Bai R; Tian L; Li Y; Zhang J; Wei Y; Jin Z; Liu Z; Liu H Combining ECM Hydrogels of Cardiac Bioactivity with Stem Cells of High Cardiomyogenic Potential for Myocardial Repair. Stem Cells Int. 2019, 2019, No. 6708435. [PubMed: 31772589]

(61). Freytes DO; O'Neill JD; Duan-Arnold Y; Wrona EA; Vunjak-Novakovic G Natural Cardiac Extracellular Matrix Hydrogels for Cultivation of Human Stem Cell-derived Cardiomyocytes. Methods Mol. Biol 2014, 1181, 69–81. [PubMed: 25070328]

(62). Kaiser NJ; Kant RJ; Minor AJ; Coulombe KLK Optimizing Blended Collagen-Fibrin Hydrogels for Cardiac Tissue Engineering with Human iPSC-derived Cardiomyocytes. ACS Biomater. Sci. Eng 2019, 5, 887–899. [PubMed: 30775432]

(63). des Rieux A; Shikanov A; Shea LD Fibrin Hydrogels for Non-viral Vector Delivery In Vitro. J. Controlled Release 2009, 136, 148–154.

(64). Juhl O IV; Zhao N; Merife AB; Cohen D; Friedman M; Zhang Y; Schwartz Z; Wang Y; Donahue H Aptamer-Functionalized Fibrin Hydrogel Improves Vascular Endothelial Growth Factor Release Kinetics and Enhances Angiogenesis and Osteogenesis in Critically Sized Cranial Defects. ACS Biomater. Sci. Eng 2019, 5, 6152–6160. [PubMed: 32190730]

(65). Burmeister DM; Roy DC; Becerra SC; Natesan S; Christy RJ In Situ Delivery of Fibrin-Based Hydrogels Prevents Contraction and Reduces Inflammation. J. Burn Care Res 2018, 39, 40–53. [PubMed: 28557870]

(66). Chung E; Rytlewski JA; Merchant AG; Dhada KS; Lewis EW; Suggs LJ Fibrin-based 3D Matrices Induce Angiogenic Behavior of Adipose-derived Stem Cells. Acta Biomater. 2015, 17, 78–88. [PubMed: 25600400]

(67). Zhao N; Suzuki A; Zhang X; Shi P; Abune L; Coyne J; Jia H; Xiong N; Zhang G; Wang Y Dual Aptamer-Functionalized in Situ Injectable Fibrin Hydrogel for Promotion of Angiogenesis via Codelivery of Vascular Endothelial Growth Factor and Platelet-Derived Growth Factor-BB. ACS Appl. Mater. Interfaces 2019, 11, 18123–18132. [PubMed: 31026135]

(68). Williams C; Budina E; Stoppel WL; Sullivan KE; Emani S; Emani SM; Black LD III Cardiac Extracellular Matrix-Fibrin Hybrid Scaffolds with Tunable Properties for Cardiovascular Tissue Engineering. Acta Biomater. 2015, 14, 84–95. [PubMed: 25463503]

(69). Mason BN; Starchenko A; Williams RM; Bonassar LJ; Reinhart-King CA Tuning three-dimensional collagen matrix stiffness independently of collagen concentration modulates endothelial cell behavior. Acta Biomater. 2013, 9, 4635–4644. [PubMed: 22902816]

(70). Wassenaar JW; Braden RL; Osborn KG; Christman KL Modulating In Vivo Degradation Rate of Injectable Extracellular Matrix Hydrogels. J. Mater. Chem. B 2016, 4, 2794–2802. [PubMed: 27563436]

(71). Hsieh FY; Tao L; Wei Y; Hsu SH A Novel Biodegradable Self-healing Hydrogel to Induce Blood Capillary Formation. NPG Asia Mater. 2017, 9, No. e363.

(72). Ehrbar M; Djonov VG; Schnell C; Tschanz SA; Martiny-Baron G; Schenk U; Wood J; Burri PH; Hubbell JA; Zisch AH Cell-demanded Liberation of VEGF121 from Fibrin Implants Induces Local and Controlled Blood Vessel Growth. Circ. Res 2004, 94, 1124–1132. [PubMed: 15044320]

(73). Kulkarni M; O'Loughlin A; Vazquez R; Mashayekhi K; Rooney P; Greiser U; O'Toole E; O'Brien T; Malagon MM; Pandit A Use of a Fibrin-based System for Enhancing Angiogenesis

and Modulating Inflammation in the Treatment of Hyperglycemic Wounds. Biomaterials 2014, 35, 2001–2010. [PubMed: 24331702]

(74). Kniebs C; Kreimendahl F; Köpf M; Fischer H; Jockenhoevel S; Thiebes AL Influence of Different Cell Types and Sources on Pre-Vascularisation in Fibrin and Agarose-Collagen Gels. Organogenesis 2020, 16, 14–26. [PubMed: 31809643]

(75). Murphy KC; Whitehead J; Zhou D; Ho SS; Leach JK Engineering Fibrin Hydrogels to Promote the Wound Healing Potential of Mesenchymal Stem Cell Spheroids. Acta Biomater. 2017, 64, 176–186. [PubMed: 28987783]

(76). Narayan R; Agarwal T; Mishra D; Maiti TK; Mohanty S Goat Tendon Collagen-Human Fibrin Hydrogel for Comprehensive Parametric Evaluation of HUVEC Microtissue-based Angiogenesis. Colloids Surf., B 2018, 163, 291–300.

(77). Richter A; Li Y; Rehbock C; Barcikowski S; Haverich A; Wilhelmi M; Böer U Triple Modification of Alginate Hydrogels by Fibrin Blending, Iron Nanoparticle Embedding, and Serum Protein-Coating Synergistically Promotes Strong Endothelialization. Adv. Mater. Interfaces 2021, 8, No. 2002015.

(78). Amado LC; Saliaris AP; Schuleri KH; St. John M; Xie JS; Cattaneo S; Durand DJ; Fitton T; Kuang JQ; Stewart G; Lehrke S; Baumgartner WW; Martin BJ; Heldman AW; Hare JM Cardiac Repair with Intramyocardial Injection of Allogeneic Mesenchymal Stem Cells after Myocardial Infarction. Proc. Natl. Acad. Sci. U.S.A 2005, 102, 11474–11479. [PubMed: 16061805]

(79). Pittenger MF; Martin BJ Mesenchymal Stem Cells and their Potential as Cardiac Therapeutics. Circ. Res 2004, 95, 9–20. [PubMed: 15242981]

(80). Ohnishi S; Yanagawa B; Tanaka K; Miyahara Y; Obata H; Kataoka M; Kodama M; Ishibashi-Ueda H; Kangawa K; Kitamura S; Nagaya N Transplantation of Mesenchymal Stem Cells Attenuates Myocardial Injury and Dysfunction in a Rat Model of Acute Myocarditis. J. Mol. Cell. Cardiol 2007, 42, 88–97. [PubMed: 17101147]

(81). Guo J; Lin GS; Bao CY; Hu ZM; Hu MY Anti-inflammation Role for Mesenchymal Stem Cells Transplantation in Myocardial Infarction. Inflammation 2007, 30, 97–104. [PubMed: 17497204]

(82). Wang X; Zhen L; Miao H; Sun Q; Yang Y; Que B; Lao EPL; Wu X; Ren H; Shi S; Lau WB; Ma X; Ma C; Nie S Concomitant Retrograde Coronary Venous Infusion of Basic Fibroblast Growth Factor Enhances Engraftment and Differentiation of Bone Marrow Mesenchymal Stem Cells for Cardiac Repair after Myocardial Infarction. Theranostics 2015, 5, 995–1006. [PubMed: 26155315]

(83). Tang Y; Gan X; Cheheltani R; Curran E; Lamberti G; Krynska B; Kiani MF; Wang B Targeted Delivery of Vascular Endothelial Growth Factor Improves Stem Cell Therapy in a Rat Myocardial Infarction Model. Nanomedicine 2014, 10, 1711–1718. [PubMed: 24941463]

(84). Bartolucci J; Verdugo FJ; González PL; Larrea RE; Abarzua E; Goset C; Rojo P; Palma I; Lamich R; Pedreros PA; Valdivia G; Lopez VM; Nazzal C; Alcayaga-Miranda F; Cuenca J; Brobeck MJ; Patel AN; Figueroa FE; Khoury M Safety and Efficacy of the Intravenous Infusion of Umbilical Cord Mesenchymal Stem Cells in Patients With Heart Failure: A Phase 1/2 Randomized Controlled Trial (RIMECARD Trial [Randomized Clinical Trial of Intravenous Infusion Umbilical Cord Mesenchymal Stem Cells on Cardiopathy]). Circ. Res 2017, 121, 1192–1204. [PubMed: 28974553]

(85). Butler J; Epstein SE; Greene SJ; Quyyumi AA; Sikora S; Kim RJ; Anderson AS; Wilcox JE; Tankovich NI; Lipinski MJ; Ko YA; Margulies KB; Cole RT; Skopicki HA; Gheorghiade M Intravenous Allogeneic Mesenchymal Stem Cells for Nonischemic Cardiomyopathy: Safety and Efficacy Results of a Phase II-A Randomized Trial. Circ. Res 2017, 120, 332–340. [PubMed: 27856497]

(86). Can A; Ulus AT; Cinar O; Celikkan FT; Simsek E; Akyol M; Canpolat U; Erturk M; Kara F; Ilhan O Human Umbilical Cord Mesenchymal Stromal Cell Transplantation in Myocardial Ischemia (HUC-HEART Trial). A Study Protocol of a Phase 1/2, Controlled and Randomized Trial in Combination with Coronary Artery Bypass Grafting. Stem Cell Rev. Rep 2015, 11, 752–760. [PubMed: 26123356]

(87). Hare JM; Traverse JH; Henry TD; Dib N; Strumpf RK; Schulman SP; Gerstenblith G; DeMaria AN; Denktas AE; Gammon RS; Hermiller JB Jr; Reisman MA; Schaer GL; Sherman W A Randomized, Double-blind, Placebo-controlled, Dose-escalation Study of Intravenous Adult

Human Mesenchymal Stem Cells (prochymal) after Acute Myocardial Infarction. J. Am. Coll. Cardiol 2009, 54, 2277–2286. [PubMed: 19958962]

(88). Guo Y; Yu Y; Hu S; Chen Y; Shen Z The Therapeutic Potential of Mesenchymal Stem Cells for Cardiovascular Diseases. Cell Death Dis. 2020, 11, No. 349. [PubMed: 32393744]

(89). Bussche L; Van de Walle GR Peripheral Blood-Derived Mesenchymal Stromal Cells Promote Angiogenesis via Paracrine Stimulation of Vascular Endothelial Growth Factor Secretion in the Equine Model. Stem Cells Transl. Med 2014, 3, 1514–1525. [PubMed: 25313202]

(90). Szaraz P; Gratch YS; Iqbal F; Librach CL In Vitro Differentiation of Human Mesenchymal Stem Cells into Functional Cardiomyocyte-like Cells. J. Visualized Exp 2017, 126, No. 55757.

(91). Yoon YS; Wecker A; Heyd L; Park JS; Tkebuchava T; Kusano K; Hanley A; Scadova H; Qin G; Cha DH; Johnson KL; Aikawa R; Asahara T; Losordo DW Clonally Expanded Novel Multipotent Stem Cells from Human Bone Marrow Regenerate Myocardium after Myocardial Infarction. J. Clin. Invest 2005, 115, 326–338. [PubMed: 15690083]

(92). Chiossone L; Conte R; Spaggiari GM; Serra M; Romei C; Bellora F; Becchetti F; Andaloro A; Moretta L; Bottino C Mesenchymal Stromal Cells Induce Peculiar Alternatively Activated Macrophages Capable of Dampening Both Innate and Adaptive Immune Responses. Stem Cells 2016, 34, 1909–1921. [PubMed: 27015881]

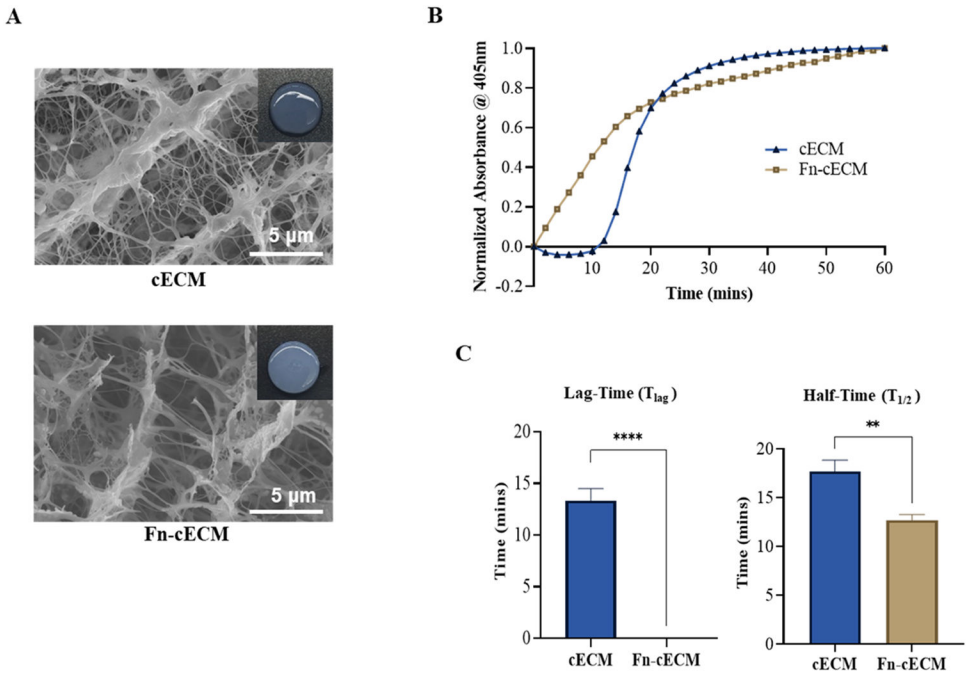

Figure 1.

Hydrogel morphology and gelation properties. (A) Macroscopic view of cardiac extracellular matrix (cECM) and hybrid (Fn-cECM) hydrogels with their respective scanning electron microscope (SEM) images. (B) Gelation kinetics of the hydrogels. (C) T_{lag} and $T_{1/2}$ of the hydrogels. Scale bar: 10 μm. $n = 3$. $^{**}p < 0.01$, $^{****}p < 0.0001$.

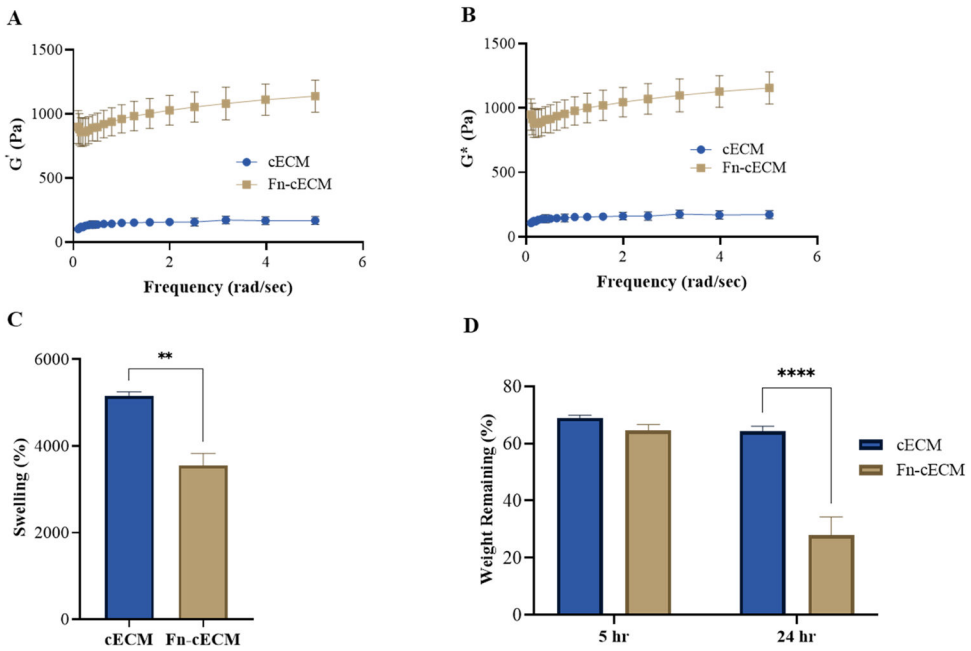

Figure 2.

Hydrogel characterization. (A) Storage moduli (G') of cECM and Fn-cECM hydrogels. (B) Complex moduli (G^*) of cECM and Fn-cECM hydrogels. $n = 5$. As $G' \gg G''$, the value of G^* is similar to G'.(C) Swelling ratios of cECM and Fn-cECM hydrogels. (D) Degradation of cECM and Fn-cECM hydrogels in collagenase type-I. $n = 3$. $^{**}p < 0.01$, $^{****}p < 0.0001$.

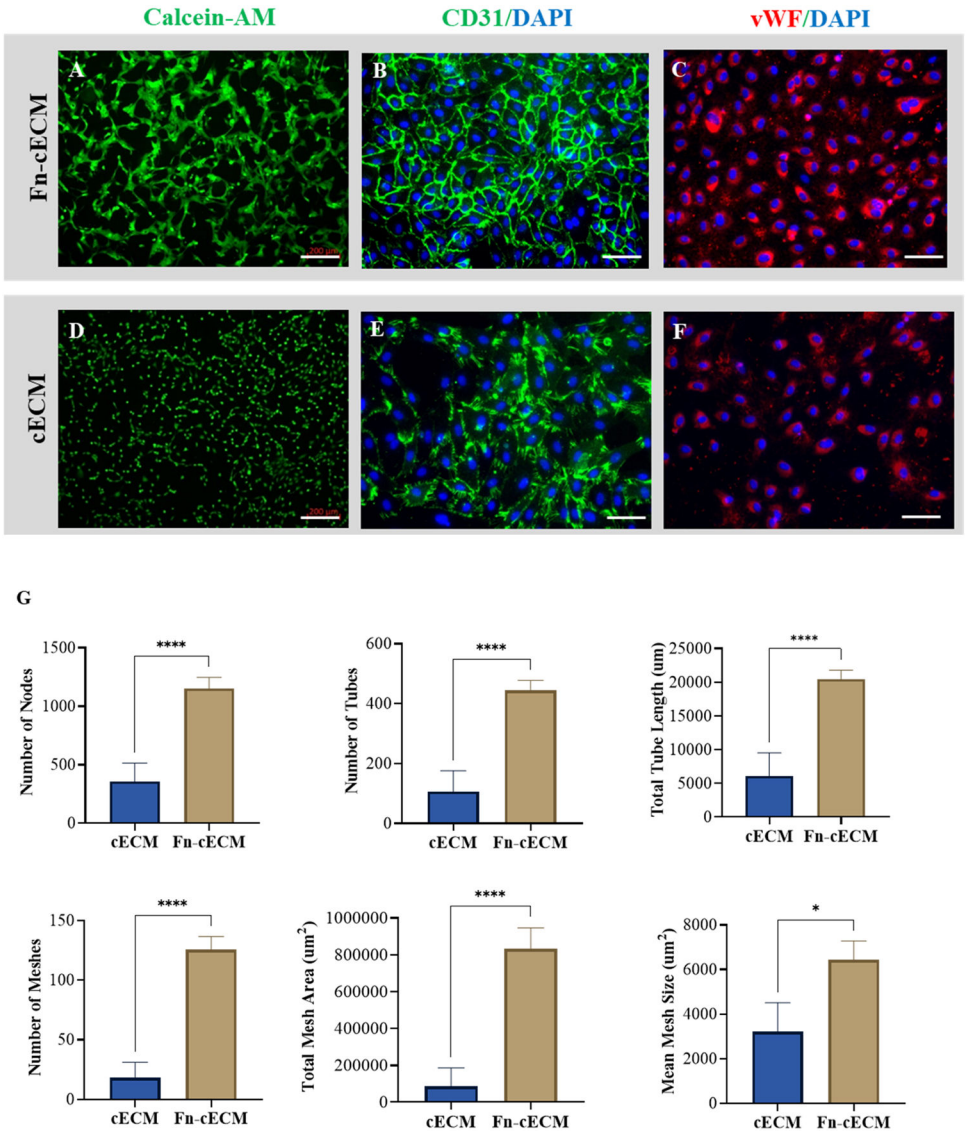

Figure 3.

Endothelial cell tube formation assay. (A, D) Vascular network formation and expression of (B, E) CD31 of HUVECs on Fn-cECM (A, B) and cECM (D, E) hydrogels. (C, F) Expression of vWF for HUVECs seeded on Fn-cECM (C) and cECM (F) hydrogels. Scale bar: 200 μm in A, D and 100 μm in B, C, E, and F. (G) Quantification of angiogenesis parameters using ImageJ software. $n = 7$; *$p < 0.05$, ****$p < 0.0001$.

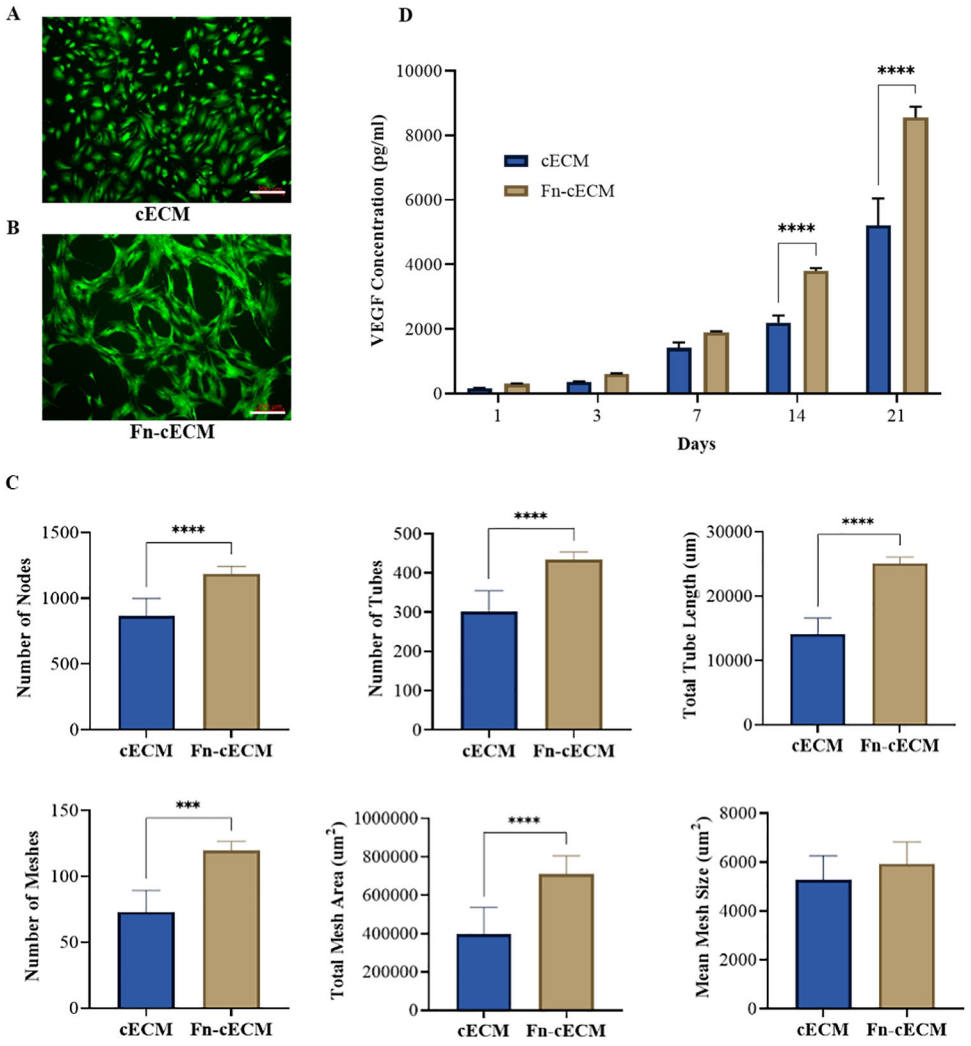

Figure 4.

Vascular network formation and VEGF secretion of hMSCs seeded on the hydrogels. (A, B) Calcein AM staining of hMSCs seeded on cECM and Fn-cECM hydrogels. Scale bar: 200 μm. (C) Quantification of angiogenesis parameters using ImageJ software. $n = 7$. (D) VEGF secreted by hMSCs seeded on cECM and Fn-cECM hydrogels quantified over a period of 3 weeks using ELISA. $n = 3$. ***$p < 0.001$, ****$p < 0.0001$.

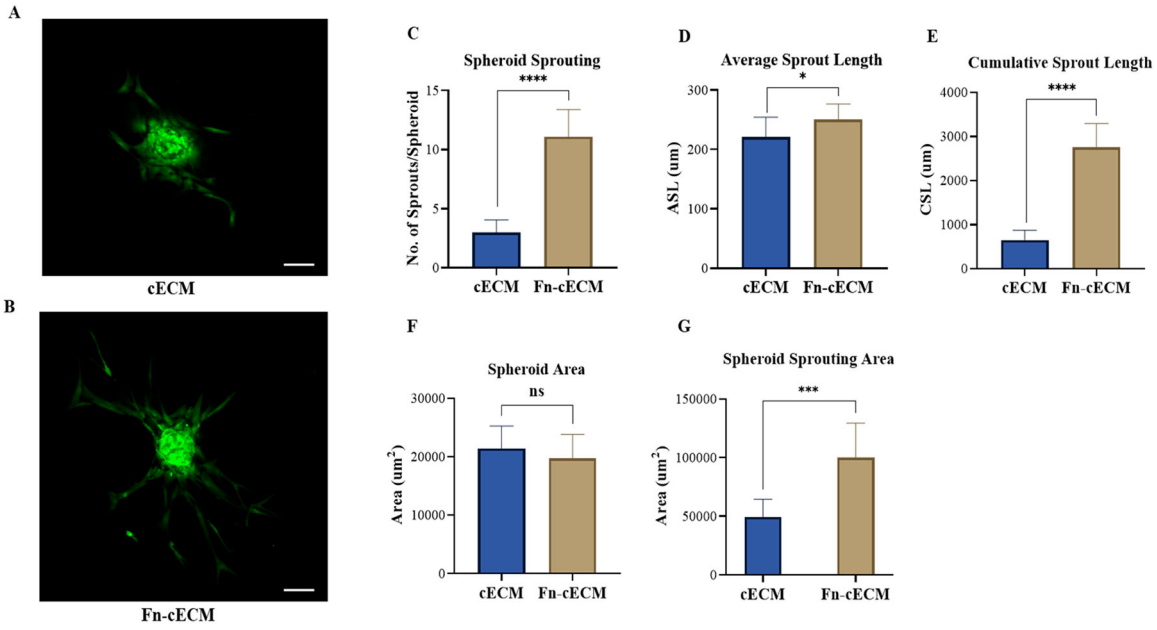

Figure 5.

Spheroid sprouting assay for hMSCs seeded on hydrogels. (A, B) Spheroid sprouting from Calcein-AM-stained hMSCs seeded on cECM and Fn-cECM hydrogels. Scale bar: 200 μm. (C–F) Quantification of spheroid sprouting using ImageJ software. $n = 10$. *$p < 0.05$, ****$p < 0.0001$.

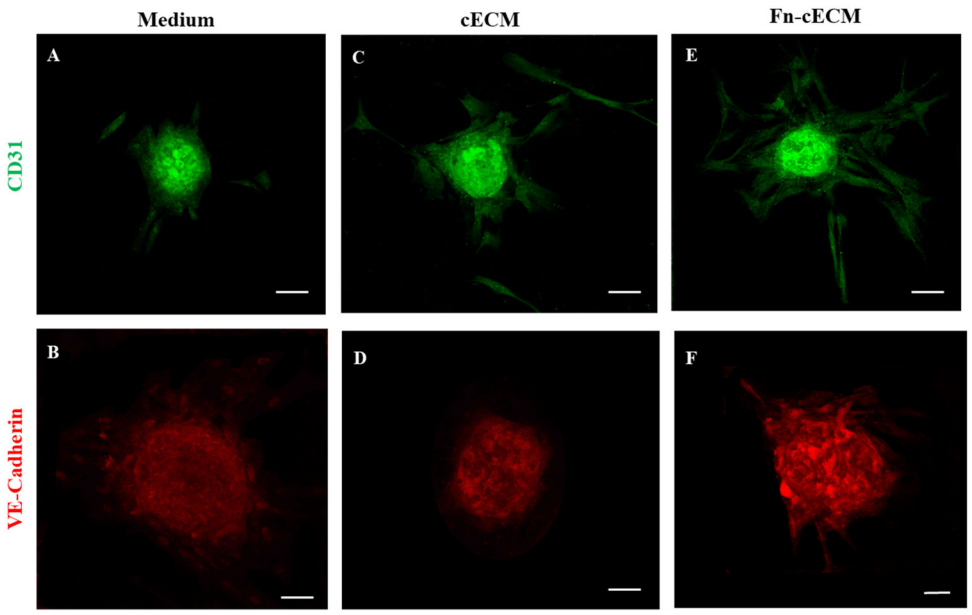

Figure 6.

Immunofluorescence staining of hMSC spheroids with endothelial cell markers CD31 (A, C, and E) and VE-Cadherin (B, D, and F) under different culture conditions. (A, B) hMSC spheroids cultured in cell medium. (C, D) hMSC spheroids cultured on cECM hydrogels. (E, F) hMSC spheroids cultured on Fn-cECM hydrogels. Scale bar: 100 μm.